 CMES, vol.48, no.3, pp.271-301, 2009

Modelling of Interfaces in Biomechanics and Mechanobiology

J. M. García-Aznar[1,2], M. A. Pérez[1,2] and P. Moreo[1,3]

Abstract: There are many interfaces between biological materials with a structural functionality, where their mechanical behaviour is crucial for their own performance. Advanced tools such as cohesive surface models are being used to simulate the failure and degradation of this kind of biological interactions. The goal of this paper, in a first step, is to present some cohesive surface models that include damage and repair in interfaces and its application to different biomechanical problems. Secondly, we discuss about the main challenges that we have to improve in the modelling of interfaces for a mechanobiological approach.

Keywords: Interface, Biomechanics, Mechanobiology.

1 Introduction

Contact mechanics is the study of the deformation of solids that touch each other at one or more points [Zhong and Mackerle (1992, 1994); Jackson and Kogut (2006); Pugliese, Tavares, Ciulli, and Ferreira (2008)]. On the other hand, an interface can be defined as the boundary between two materials or solids, therefore it may be considered as a contact problem. In Engineering there are many examples involving interfaces (composite materials, concrete, metals, etc.) that have been modelled using cohesive interface models [Irwin, Kies, and Smith (1958); Needleman (1987, 1990); Camacho and Ortiz (1996); Chandra and Shet (2004); Li and Siegmund (2004); Cocchetti, Maier, and Shen (2002)]. However, there are other application fields, such as in Biomechanics and Mechanobiology, where many examples of interfaces are also found: growth plate of long bones, bone-tendon interface, dentine-enamel interface, cartilage-bone interface, tooth-host bone, etc. The role

[1] Group of Structural Mechanics and Materials Modelling (GEMM), Aragón Institute of Engineering Research (I3A), Universidad de Zaragoza, Spain
[2] Centro de Investigación Biomédica en Red en Bioingeniería, Biomateriales y Nanomedicina (CIBER-BBN), Aragon Health Sciences Institute
[3] EBERS Medical Technology S.L., Zaragoza, Spain

of an interface is more important when there is a need to incorporate an implant or scaffold (tissue engineering). The success of this kind of implantation highly depends on the bonding interface between the biological tissue and the biomaterial. High failure rates of implants and scaffolds are produced at the interface between both materials. Therefore, characterization of the failure mechanisms of these interfaces is a key in the biomechanics field.

For example, it is evident that the placement of an implant inside bone gives rise to the appearance of interfaces, whose nature will depend on the type of implant in question:

- In cemented implants, there exists a cement layer between the implant and the bone. Therefore, two different interfaces can be distinguished: the cement-bone and the cement-implant interface.
- In the case of cementless implants only one new interface appears: the bone-implant interface.

It is important to notice that the main features and most relevant phenomena that take place at each of the three previously mentioned interfaces vary significantly depending on the type of interface. Clearly, the cement-implant interface is the boundary between two nonbiological materials and thus, from a biological standpoint, can be considered as an inert interface. On the other hand, both the cement-bone and the bone-implant interfaces separate an inert solid surface from a biological environment, and commonly receive the name of biological interfaces [Kasemo (1998)]. While at inert interfaces it can be expected that mechanical processes play a relevant role, at the interface between a solid material surface and its biological environment a vital ingredient is to understand, control and optimise the biological and physicochemical interactions occurring between the two. In any case, the study of implant interfaces is an issue of the utmost importance for the design of bone implants, since they strongly influence their long-term outcome.

For instance, the cement-implant interface can be the point of origin of the mechanical debonding of cemented implants [Jasty, Maloney, Bragdon, O'Connor, Haire, and Harris (1991); Fornasier and Cameron (1976); Harris (1992)]. In particular, the surface finishing of the implant affects the mechanical behaviour of the cement-implant interface and is a controversial parameter of design. While some authors defend that a stiffening of this interface thanks to the use of a rougher implant surface finishing can postpone the loosening of the implant [Stone, Wilkinson, and Stother (1989); Harris (1992)], others maintain that a polished surface yields better clinical results since it reduces the problem of osteolysis originated by particle detachment, typically associated to rougher implant surfaces [Huiskes,

Verdonschot, and Nivbrant (1998); Collis and Mohler (2002); Pérez, García-Aznar, Doblaré, Seral, and Seral (2006)]. In the case of the cement-bone interface, albeit being a biological interface, it is also worth to study its mechanical behaviour, since this interface is another possible point for the initiation of the debonding of cemented implants [Mohler, Callaghan, Collis, and Johnston (1995); Race, Miller, Ayers, and Mann (2003)]. Actually its mechanical behaviour is highly nonlinear, involving loss of stiffness, appearance of plastic deformations and fatigue, among other effects [Kim, Miller, and Mann (2004b,a)].

An example of a different type of interface is the bone-implant interface where its fixation depends on the deposition of new bone matrix on the surface of the implant. This process is the result of a series of biological events [Davies (2003)], that can be regulated by biological and mechanical factors. Here a new field is involved, mechanobiology, which aims to investigate how mechanical forces modulate morphological and structural fitness of the skeletal tissues (bone, cartilage, ligament and tendon) [van der Meulen and Huiskes (2002)]. How the bone regenerates or renews at the implant surface depends on how cells responsed to the mechanical stimuli. Most of computational studies have considered two possible configurations of these interfaces, completely bonded or completely debonded with/without friction [Mann, Bartel, Wright, and Burstein (1995); Lennon and Prendergast (2001); Stolk, Verdonschot, and Huiskes (2001); Van Oosterwyck, Duyck, Vander Sloten, Van der Perre, Cooman, Lievens, Puers, and Naert (1998)], neglecting the evolutive process of interface deterioration or regeneration. The incorporation of a cohesive interface model may help to understand the complex interactions here involved. Therefore, the main goal of the present study is related with the complex behaviour of the interfaces located in biological tissues or between these and implants. Advanced tools as cohesive surface models are proposed to be used in order to simulate the failure, degradation or regeneration of these kind of biological surfaces. In section 2 and 3, the main differences on modelling interfaces in biomechanics and mechanobiology will be discussed, respectively. Finally, the main conclusions will be presented in section 4.

2 Interfaces in Biomechanics

There are many interfaces in the human body with a mechanical role. When their mechanical failure occurs, it produces the partial or total collapse of a region and a complicated clinical problem is produced.

One of the most important problems is related with the lack of experimental measurements, which makes difficult to choose about the most adequate cohesive constitutive law for each interface. This fact necessitates the need to apply simplified assumptions. In this section, a simplified damage interface cohesive model is pre-

sented [Moreo, Pérez, García-Aznar, and Doblaré (2006)] which could be applied to different biomechanical problems. Just to show one application, this model has been applied to simulate the failure of the growth plate in long bones [Gómez-Benito, Moreo, Pérez, Paseta, García-Aznar, Barrios, and Doblaré (2007)].

2.1 Modelling deterioration of interfaces

In this section, a model able to account for the mechanical degradation of an interface is presented [Moreo, Pérez, García-Aznar, and Doblaré (2006)] and its potential is shown in an example of clinical interest.

2.1.1 Mathematical formulation of the model

General framework. Constitutive equations

To model the interface behaviour, a cohesive zone model with constitutive equations based on Continuum Damage Mechanics has been used. Accordingly, the model is established in terms of the interface relative displacements $\boldsymbol{\delta}$ (also referred to as the jump of displacements across the interface) and the interface tractions $\mathbf{t}$. We define a local reference system at the interface considering the 1-axis as the normal direction to the interface and the 2 and 3-axis as the tangential directions (see Fig. 1).

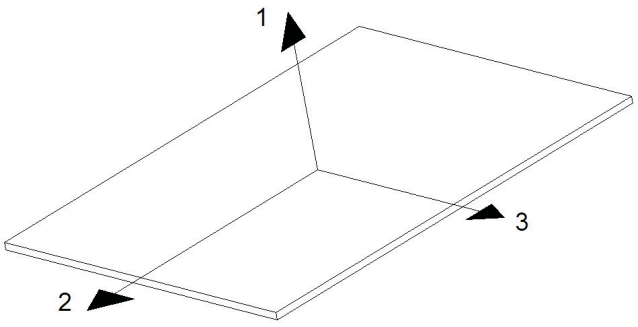

Figure 1: Local reference system at the interface.

Only isothermal processes are considered and the hypothesis of small displacements is admitted. Thus, the state variables are the total displacement vector $\boldsymbol{\delta}$ and a single scalar damage variable d. To define the constitutive equations, the Helmholtz free energy function ψ is used as thermodynamical potential:

$$\psi(\boldsymbol{\delta}, d) = \frac{1}{2}\boldsymbol{\delta} \cdot [\mathbf{I} - d\mathbf{C}]\mathbf{K}\boldsymbol{\delta} \tag{1}$$

where $\mathbf{I}$ is the identity matrix, $\mathbf{K}$ is the undamaged stiffness matrix

$$\mathbf{K} = \begin{bmatrix} K_{01} & 0 & 0 \\ 0 & K_{02} & 0 \\ 0 & 0 & K_{03} \end{bmatrix} \tag{2}$$

$\mathbf{C}$ is defined as

$$\mathbf{C} = \begin{bmatrix} h(\delta_1) & 0 & 0 \\ 0 & 1 & 0 \\ 0 & 0 & 1 \end{bmatrix} \tag{3}$$

$$h(x) = \begin{cases} 1 & \text{if} \quad x \geq 0 \\ 0 & \text{if} \quad x < 0 \end{cases}$$

As it will be proved later, the inclusion of matrix $\mathbf{C}$ and the definition of $h(\delta_1)$ imply that, first, under compressive loads the effective normal stiffness is always the corresponding to the undamaged situation, whatever the value of damage d is, what accounts for the well-known phenomenon of crack closure. Secondly, damage does not increase under compression, what accounts for the intuitive idea that the magnitude of the compression load that would cause mechanical deterioration of the interface is very large compared to physiological loads that appear in usual conditions.

From the Claussius-Duhem inequality, assuming elastic unloading and using standard arguments in Continuum Mechanics, the following classical expressions can be obtained [Coleman and Gurtin (1967); Coleman and Noll (1963)]:

$$\mathbf{t} = \frac{\partial \psi}{\partial \boldsymbol{\delta}} = [\mathbf{I} - d\mathbf{C}]\mathbf{K}\boldsymbol{\delta} \tag{4a}$$

$$Y = -\frac{\partial \psi}{\partial d} = \frac{1}{2}\boldsymbol{\delta} \cdot \mathbf{C}\mathbf{K}\boldsymbol{\delta} \tag{4b}$$

where $\mathbf{t}$ denotes the interface traction vector and Y the thermodynamic driving force conjugated to the damage variable d.

Note that from the examination of Eq.4a it is straightforwardly inferred that, under compression ($\delta_1 < 0$), the normal traction always takes the value $t_1 = K_{01}\delta_1$, irrespective of the value of d. For the subsequent development of the model, it will be

necessary to decompose Y as the sum of two directional contributions Y_N (normal) and Y_T (tangential):

$$Y = Y_N + Y_T$$

where

$$Y_N = \frac{1}{2} h(\delta_1) K_{01} \delta_1^2 \tag{5a}$$

$$Y_T = \frac{1}{2} (K_{02} \delta_2^2 + K_{03} \delta_3^2) \tag{5b}$$

Damage characterization

The main feature of the proposed damage model lies in the fact that there exist two different evolution mechanisms for the single scalar damage variable d, associated to normal and shear loading, respectively. Each mechanism has an associated damage criterion and the evolution of d is established in terms of the mechanism that leads to a greater increase of d.

The same behaviour in any tangential direction was assumed. Therefore, in the damage characterization of the interface it is not necessary to distinguish between the two tangential directions. The formulation is therefore established in terms of the normal and the total tangential components of the interface traction vector and the corresponding relative displacements, which will be denoted in the following by subscripts $(\cdot)_N$ and $(\cdot)_T$, respectively.

Some of the experimental studies described in the Introduction could be modelled through a law with an initial linear behaviour followed by an exponential decay. Based on this observation, the following relation between ultimate tractions t_β^u and relative displacements δ_β is proposed (see Fig. 2):

$$t_\beta^u = \begin{cases} A_\beta e^{B_\beta \delta_\beta} + C_\beta & \text{if } 0 \le \delta_\beta < \delta_{c\beta} \\ 0 & \text{if } \delta_{c\beta} \le \delta_\beta \end{cases} \qquad \beta = N, T \tag{6}$$

where $\delta_{c\beta}$ stands for the displacement corresponding to total failure and $A_\beta > 0$, $B_\beta < 0$ and $C_\beta < 0$ are constants dependent on the specific mechanical properties of the interface. A_β, B_β and C_β can be written in terms of four alternative more physical mechanical properties in each direction (see Fig. 2): $\delta_{0\beta}$ (maximum relative displacement in the linear region, displacement at ultimate stress), $G_{c\beta}$ (critical failure energy), $t_{0\beta}$ (apparent strength) and $\delta_{c\beta}$ (displacement at breakpoint).

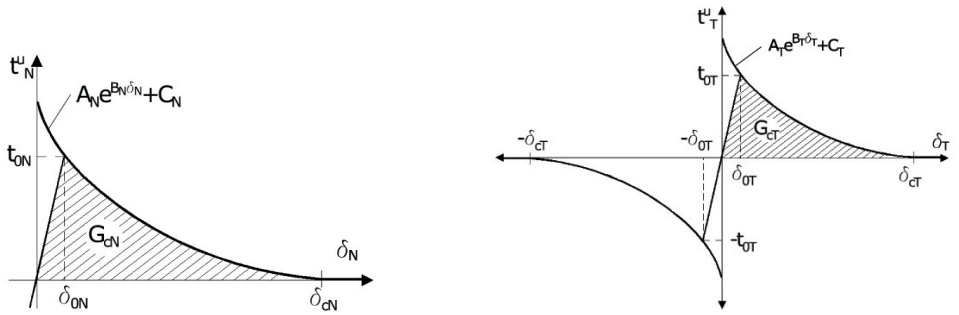

(a) (b)

Figure 2: Ultimate strength-relative displacement curve: (a) Normal direction (b) Shear direction (with permission from Moreo, Pérez, García-Aznar, and Doblaré (2006)

The expressions that relate $A_\beta > 0$, $B_\beta < 0$ and $C_\beta < 0$ with $\delta_{0\beta}$, $G_{c\beta}$, $t_{0\beta}$ and $\delta_{c\beta}$ can be derived as follows:

- When one sets $\delta_\beta = \delta_{0\beta}$ in Eq.6, the ultimate interface traction should correspond to the apparent strength $t_{0\beta}$; and when the relative displacement δ_β is set to the maximum relative displacement $\delta_{c\beta}$, then the ultimate traction should be null. From these conditions, the following expression for A_β is determined:

$$A_\beta = \frac{t_{0\beta}}{e^{B_\beta \delta_{0\beta}} - e^{B_\beta \delta_{c\beta}}} \qquad \beta = N,T \tag{7}$$

- The critical failure energy $G_{c\beta}$ is the area under the traction/relative displacement curve for the single mode β (Fig. 2) and thus

$$G_{c\beta} = G_{0\beta} + \int_{\delta_{0\beta}}^{\delta_{c\beta}} (A_\beta e^{B_\beta \delta_\beta} + C_\beta) d\delta_\beta \qquad \beta = N,T \tag{8}$$

Being $G_{0\beta}$ the area under the first linear branch of the traction/relative displacement curve, that is

$$G_{0\beta} = \frac{1}{2} K_{0\beta} \delta_{0\beta}^2 \qquad \beta = N,T \tag{9}$$

- B_β can be computed by solving the nonlinear equation that results after substituting Eq.7 into 8 and evaluating the integral.
- Finally, once that A_β and B_β are known, C_β can be trivially calculated from

$$C_\beta = t_{0\beta} - A_\beta e^{B_\beta \delta_{0\beta}} \qquad \beta = N,T \tag{10}$$

Now, a damage criterion for each mechanism will be established by means of the yield functions f_β, which obviously depend on the definition of t_β^u:

$$f_\beta(Y_\beta, d) = (1-d)\sqrt{2K_{0\beta}Y_\beta} - t_\beta^u\left(\sqrt{\frac{2Y_\beta}{K_{0\beta}}}\right) \qquad \beta = N,T \tag{11}$$

where $K_{0N} = K_{01}$ and $K_{0T} = K_{02} = K_{03}$.

Next, the evolution of damage d is computed as

$$\dot{d} = \max\left\{\mu_N \frac{\partial f_N}{\partial Y_N}, \mu_T \frac{\partial f_T}{\partial Y_T}\right\} \tag{12}$$

being μ_N and μ_T the consistency parameters.

The loading/unloading conditions (usually referred as Kuhn-Tucker conditions in mathematical programming literature [Luenberger (1984)]) can be written as

$$\mu_\beta \geq 0; \quad f_\beta \leq 0; \quad \mu_\beta f_\beta = 0 \qquad \beta = N,T \tag{13}$$

It can be seen that, under normal compression loads ($\delta_1 < 0$), the corresponding driving force $Y_N = 0$ (Eq.5a) and the normal damage evolution mechanism is never activated, since $f_N < 0$.

Moreover, the consistency condition establishes that, in the case of loading with a certain damage mechanism β activated, the relationship $\mu_\beta \dot{f}_\beta = 0$ is fulfilled. This condition allows to obtain the following expressions for the consistency parameters (recall that $\delta_T = \sqrt{\delta_2^2 + \delta_3^2}$):

$$\mu_N = \dot{\delta}_1 \tag{14a}$$

$$\mu_T = \frac{\delta_2\dot{\delta}_2 + \delta_3\dot{\delta}_3}{\sqrt{\delta_2^2 + \delta_3^2}} = \dot{\delta}_T \tag{14b}$$

Finally, taking into account (14a) and (14b), the evolution of the tractions can be written as

$$\dot{\mathbf{t}} = \mathbf{K}^d \dot{\boldsymbol{\delta}} \tag{15}$$

where

$$\mathbf{K}^d = \begin{cases} [\mathbf{I} - d\mathbf{C}]\mathbf{K} & \text{if} \quad \mu_N = \mu_T = 0 \\ [\mathbf{I} - d\mathbf{C}]\mathbf{K} - \dfrac{\partial f_*}{\partial Y_*}\mathbf{C}\mathbf{K}\boldsymbol{\delta} \cdot \dfrac{(\mathbf{H}_*\boldsymbol{\delta})^\top}{\sqrt{(\mathbf{H}_*\boldsymbol{\delta})^\top (\mathbf{H}_*\boldsymbol{\delta})}} & \text{otherwise} \end{cases} \tag{16}$$

where the subscript $(\cdot)_*$ denotes the damage evolution mechanism, normal or tangential, that at a precise moment is leading to a greater value of $\dot{d}$ (see Eq. 12) and $\mathbf{H}_*$ is defined as

$$\mathbf{H}_* = \begin{cases} \begin{bmatrix} 1 & 0 & 0 \\ 0 & 0 & 0 \\ 0 & 0 & 0 \end{bmatrix} & \text{if} \quad * = N \\ \begin{bmatrix} 0 & 0 & 0 \\ 0 & 1 & 0 \\ 0 & 0 & 1 \end{bmatrix} & \text{if} \quad * = T \end{cases} \tag{17}$$

Computational implementation

An update procedure for the variables $\mathbf{t}, d$ consistent with the constitutive model is established. In this process a strain-driven approach is followed so the history of the jump of displacements at the interface is assumed to be given. The equations of evolution for damage are solved incrementally over a sequence of given time steps $[t_n, t_{n+1}] \subset \mathbb{R}^+, n = 0, 1, 2, \ldots$. Therefore, the proposed algorithm consists of the next three steps, of which the first two must be performed in each direction, normal and shear:

Step 1 Check the damage criteria

$$\textbf{if} \quad f_\beta(Y_{\beta,n+1}, d_n) \leq 0 \quad \textbf{then} \quad \widetilde{d}_{\beta,n+1} = d_n, \ \textbf{go to Step 3} \tag{18}$$

where $\widetilde{d}_{\beta,n+1}$ are auxiliary variables defined in each direction β. Otherwise, damage takes place and d is updated in **Step 2**.

Step 2 Update damage by means of equation

$$\widetilde{d}_{\beta,n+1} = 1 - \frac{t^u_\beta(\delta_{\beta,n+1})}{K_{0\beta}\,\delta_{\beta,n+1}} \tag{19}$$

Step 3 First compute the maximum between the two directional damage variables

$$\widetilde{d}_{n+1} = \max\{\widetilde{d}_{N,n+1}, \widetilde{d}_{T,n+1}\} \tag{20}$$

Then, if no cyclic loading is taking place $d_{n+1} = \widetilde{d}_{n+1}$. Otherwise, the fatigue evolution of damage must be computed by means of an appropriate law.

Finally, the stress vector $\mathbf{t}_{n+1}$

$$\mathbf{t}_{n+1} = [\mathbf{I} - d_{n+1}\mathbf{C}]\mathbf{K}\delta_{n+1} \tag{21}$$

so the whole set of n variables is updated.

2.1.2 Example of application

Slipped capital femoral epiphysis (SCFE) is a failure process in which slippage of two parts of the femur is produced at its growth plate in the hip joint. It occurs in 5 of 100.000 children from 10 to 15 years old [Canale (2003); Loder (1996, 1998)]. The early diagnosis of SCFE is difficult, because symptoms are in general unclear and radiographic diagnosis in cases of mild slip can be subtle. Therefore, it is very important to identify the patients with a higher risk of developing SCFE and computational methods could be an alternative tool to predict this pathology [Gómez-Benito, Paseta, García-Aznar, Barrios, Gascó, and Doblaré (2006); Fishkin, Armstrong, Shah, Patra, and Mihalko (2006)].

Hence, one computational study has used the previous damage interface model to simulate the SCFE process with the corresponding mechanical properties of the growth plate [Gómez-Benito, Moreo, Pérez, Paseta, García-Aznar, Barrios, and Doblaré (2007)]. The main goal is to estimate the shear/tensile strength that could be determinant to early illness prediction.

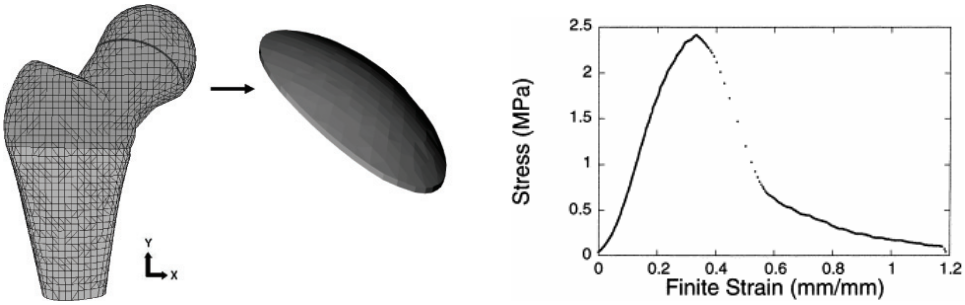

(a) (b)

Figure 3: (a) Finite element mesh of the hip with a detail of the growth plate; (b) Stress-strain curve under tension in a sheep growth plate [Williams, Do, Eick, and Schmidt (2001)]

Two parametrised geometries of the proximal femur (one of a "standard" healthy child and a "standard" affected child) including the epiphyseal growth plate was defined and validated in a previous work in order to develop a patient-specific finite element (FE) model to analyze SCFE [Paseta, Gómez-Benito, García-Aznar, Barrios, and Doblaré (2007)] (Fig. 3a). The stress-strain curve that helps to define the growth plate mechanical properties was experimentally obtained (Fig. 3b) by Williams, Do, Eick, and Schmidt (2001).

β	$\delta_{0\beta}$ (mm)	$\delta_{c\beta}$ (mm)	$t_{0\beta}$ (MPa)	$G_{c\beta} \cdot 10^{-3}$ (J/mm^2)
Tangential (T)	0.92	1.6	[0.5, 4]*	[0.32, 2.52]*
Normal (N)	0.34	1.1	[0.5, 4]*	[0.18, 1.44]*

Table 1: Parameters of the interface damage model [Williams, Vani, Eick, Petersen, and Schmidt (1999); Williams, Do, Eick, and Schmidt (2001); Cohen, Chorney, Phillips, Dick, Buckwalter, Ratcliffe, and Mow (1992); Lee, Pelker, Rudicel, Ogden, and Panjabi (1985)] (* Range of variation of the parameter analyzed in the simulations).

Due to the uncertainty of the mechanical properties of the growth plate, these were varied as shown in Table 1 in order to predict the possible failure of the growth plate, analyzing different loads corresponding to normal activities of a child [Gómez-Benito, Moreo, Pérez, Paseta, García-Aznar, Barrios, and Doblaré (2007)]. From the FE analysis, the range of values of ultimate tensile and shear stress for which slippage of the growth is expected for a specific geometry and body weight can be graphically represented. One example is illustrated in Fig. 4a, where each point of the failure curve was obtained fixing the ultimate shear stress and reducing

the ultimate tensile stress until the growth plate was not able to bear the external load. This curve allows to determine if a femur is likely or not to suffer SCFE, once a certain physiological range for the ultimate mechanical properties (dark area in Fig. 4b) is fixed.

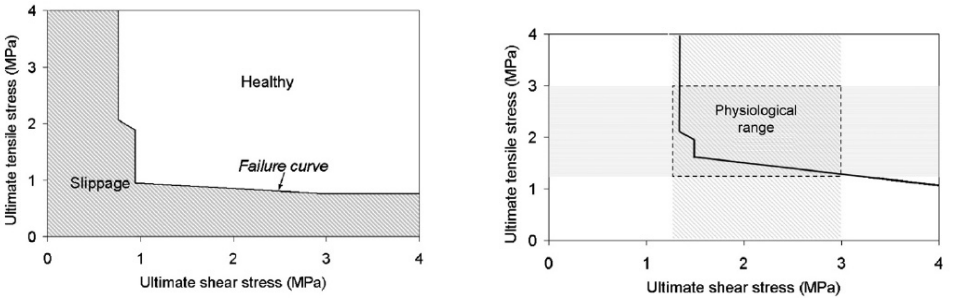

(a) (b)

Figure 4: (a) Scheme of the damage curve indicating the combination of ultimate tensile and shear stresses that separated the cases of healthy and slipped hips. (b) Gray areas represent the physiological range (with permission from [Gómez-Benito, Moreo, Pérez, Paseta, García-Aznar, Barrios, and Doblaré (2007)]

The different failure curves after simulating the healthy and the affected "standard" femora have been represented in Fig. 5. It can be observed that in the estimated physiological range for a human growth plate [1.25 MPa, 3.00 MPa] in shear and in tension the affected "standard" hip will suffer SCFE. In contrast, the healthy standard femur probably will not suffer slippage. For all combinations of ultimate tensile and shear stresses, slippage of the affected hip is more likely to occur.

Therefore, the damage model used herein demonstrates that in a reasonably physiological range of ultimate mechanical properties of the growth plate, the "standard" affected femur would damage with a higher probability than the one defined by means of geometrical parameters of healthy children with the same body weight. Thus, this model can easily help to select the subjects with a higher probability of slippage despite the uncertainties of the growth plate mechanical properties.

3 Interfaces in Mechanobiology

As presented in Section 2, modelling interfaces in biomechanics allows one to analyze the failure process of the interface once its structure and mechanical properties are known. But, normally these interfaces have unknown mechanical properties and microstructure, and they can evolve with time depending on the mechanical

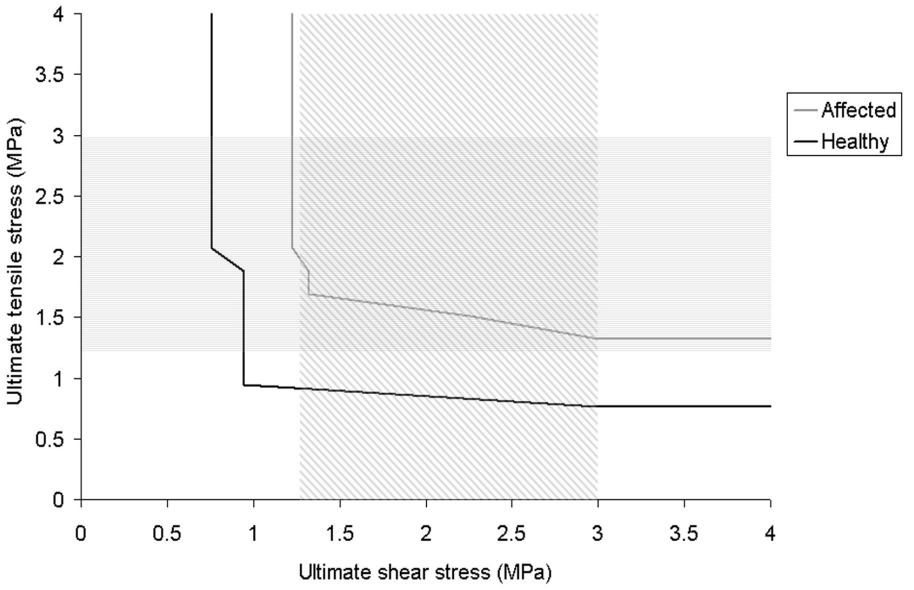

Figure 5: Damage curves for the healthy and affected "standard" femora. Gray areas represent the physiological range (with permission from [Gómez-Benito, Moreo, Pérez, Paseta, García-Aznar, Barrios, and Doblaré (2007)].

state. An example is the case of an implant or prosthesis which is attached directly to bone. At the first moment, just after implantation, the mechanical properties of the interface between the biological tissue and the biomaterial are limited. But, as time evolves and if the mechanical environment is adequate, the strength of the interface improves, and the interface becomes able to support larger loads with less motion. This regeneration process is called osseointegration, which is complex and mainly depends on biological and mechanical factors. In fact, if the mechanical stimulus is not adequate during the regeneration process, then a fibrous bonding will take place which is very flexible and not able to bear the external loads. Therefore, when an implant, prosthesis or scaffold is implanted, this kind of problems should be avoided. There are also many additional elements that can wield a significant influence on the osseointegration: biomaterial, implant surface properties, quality of surrounding bone, etc.

There are two different approaches to model this kind of problems: phenomenological and mechanistic models. The phenomenological approach predicts the formation or not of bone ingrowth as a function of mathematical expressions that

relate the mechanical stimulus and the tissue response. Phenomenological models are characterised by using simple expressions to model the formation of new bone and the associated evolution of the interface mechanical properties. For example, some authors have simulated bone ingrowth in a very simplified manner by means of finite element simulations in which the displacements of adjacent nodes of bone and implant are tied in regions of the interface where relative micromotions do not exceed a threshold value [Fernandes, Folgado, Jacobs, and Pellegrini (2002); Andreykiv, Prendergast, van Keulen, Swieszkowski, and Rozing (2005)]. These models only consider two extreme conditions: complete bonding and complete debonding with friction. Therefore, osseointegration is assumed to take place instantaneously, with a sudden jump in the mechanical properties of the interface. There exist more refined models of this type in which the mechanical properties at the bone-implant interface evolve in time according to a phenomenological law depending on the mechanical state (stress and/or strain). For instance, the model of Büchler [Büchler, Pioletti, and Rakotomanana (2003)], proposed for the simulation of hip implants. In Section 3.1, a phenomenological model for living interfaces is described.

On the other hand, mechanistic models are a step forward, in which the most important biological phenomena involved in peri-implant bone healing are explicitly modelled [Moreo, García-Aznar, and Doblaré (2009a,b)], sometimes in terms of the mechanical conditions of the environment [Geris, Andreykiv, Oosterwyck, Sloten, van Keulen, Duyck, and Naert (2004); Ambard and Swider (2006); Liu and Niebur (2008)].

3.1 Modelling living interfaces: a phenomenological approach

A phenomenological model that captures the evolutive mechanical behaviour of the bone-implant interface is presented herein. The core idea of the model is that, in spite of the complexity of the biological phenomena governing bone ingrowth, the scenario is greatly simplified if it is contemplated from a strict macroscopic mechanical standpoint:

- Under high mechanical loads, the formation of fibrous tissue is fostered and the already formed bone is damaged. This provokes a decrease in the mechanical properties (stiffness, strength) of the interface.
- Under low mechanical loads, osteogenic cells tend to differentiate into osteoblasts, which produce bone. From a mechanical point of view this involves an increase in the interface mechanical properties.
- In a situation of medium mechanical stimulation, we can assume that the

mechanical properties of the interface remain constant.

This suggests that a model for the bone-implant interface can be formulated assuming that the temporal evolution of the mechanical properties only depends on the mechanical state of the tissue. Obviously, such a model will neglect any biological influence, so its application will be restricted to specific situations in which mechanics turns out to be the main factor controlling bone formation around implants [Moreo, Pérez, García-Aznar, and Doblaré (2006)].

In particular, Moreo, Pérez, García-Aznar, and Doblaré (2006) proposed the use of a combined theory of damage-repair that, is based on the well-known theory of Continuum Damage Mechanics (CDM). It is assumed that the evolution of the internal variable (damage, d) that accounts for the interface mechanical properties can be formulated on the basis of an extension of CDM, characterised by the fact that internal variables are no longer constrained to evolve only in one direction —remember the typical conditions $\dot{d} \geq 0$ of CDM—, but can increase or decrease according to a pair of criteria. In our model, the internal variable is able to increase, representing the gain in mechanical properties that takes place at the bone-implant interface when new bone forms at the implant surface, but also to decrease, accounting for the loss of mechanical properties associated to damage of bone, due to monotonic or cyclic loading. Therefore, we can say that this model is a generalized approach that considers the option of damage and repair in the same model. Then the model for damage presented in subsection 2.1 is really a simplification of this general approach here presented.

3.1.1 Mathematical formulation of the model

General framework. Constitutive equations

The general framework of this model is equivalent to the one presented in Section 2.1.1. A cohesive zone model is formulated where the interface behaviour is again established in terms of the interface relative displacement $\boldsymbol{\delta}$ and the traction vector $\mathbf{t}$. The same local reference system defined at each point of the interface with the 1-axis normal to the interface and the 2 and 3-axis in tangential directions is also used.

Under the common assumption of an isothermal process and the hypothesis of small displacements, the state variables are the relative displacement vector $\boldsymbol{\delta}$ and a scalar internal variable α, which characterizes the degree of bonding of the interface, being normalised between 0 and 1. $\alpha = 0$ corresponds to a totally debonded interface with null stiffness and $\alpha = 1$ to a completely osseointegrated interface with maximum stiffness [1]. As it will remain evident throughout the work, this redefinition of

[1] Note that the internal variable α is just the counterpart of damage d in the model of the previous

the internal variable is preferable to gain consistency with the terminology associated to the extra additional features that this model is able to reproduce.

The Helmholtz free energy function ψ takes the following form

$$\psi(\boldsymbol{\delta},\alpha)=\frac{1}{2}\boldsymbol{\delta}\cdot[\mathbf{I}-(1-\alpha)\mathbf{C}]\mathbf{K}\boldsymbol{\delta} \tag{22}$$

where $\mathbf{I}$ is the identity matrix, $\mathbf{K}$ is the stiffness matrix in a situation of perfect bond:

$$\mathbf{K}=\begin{bmatrix} K_{01} & 0 & 0 \\ 0 & K_{02} & 0 \\ 0 & 0 & K_{03} \end{bmatrix} \tag{23}$$

and $\mathbf{C}$ is defined as

$$\mathbf{C}=\begin{bmatrix} h(\delta_1) & 0 & 0 \\ 0 & 1 & 0 \\ 0 & 0 & 1 \end{bmatrix} \tag{24}$$

$$h(x)=\begin{cases} 1 & \text{if} \quad x\geq 0 \\ 0 & \text{if} \quad x<0 \end{cases}$$

From the Claussius-Duhem inequality, assuming elastic unloading and using standard arguments in Continuum Mechanics, the following expressions are obtained [Coleman and Noll (1963); Coleman and Gurtin (1967)]:

$$\mathbf{t}=\frac{\partial\psi}{\partial\boldsymbol{\delta}}=[\mathbf{1}-(1-\alpha)\mathbf{C}]\mathbf{K}\boldsymbol{\delta} \tag{25a}$$

$$Y=\frac{\partial\psi}{\partial\alpha}=\frac{1}{2}\boldsymbol{\delta}\cdot\mathbf{C}\mathbf{K}\boldsymbol{\delta} \tag{25b}$$

where $\mathbf{t}$ denotes the interface traction vector and Y the thermodynamic driving force conjugated to the bonding degree α, which admits the standard decomposition in two directional contributions, Y_N (normal) and Y_T (tangential):

section in the sense that we can interpret α as $1-d$

$$Y = \underbrace{\frac{1}{2}h(\delta_1)K_{01}\delta_1^2}_{Y_N} + \underbrace{\frac{1}{2}(K_{02}\delta_2^2 + K_{03}\delta_3^2)}_{Y_T}$$

It is noteworthy to remark that, from a thermodynamic perspective, the bone ingrowth phenomena is completely different from the purely mechanical damage process for non-living materials. To clarify this, it is useful to understand the meaning of the product $Y\dot{\alpha}$. In mathematical models of non-living interfaces, such as those proposed in Section 2.1.1., or in the case of this model when we consider the situation of damage ($\dot{\alpha} < 0$), the product of the thermodynamic force and the temporal derivative of the internal variable has the well-known physical meaning of rate of energetic dissipation per unit volume due to the progressive failure process taking place at the material and $Y\dot{\alpha} < 0$. On the other hand, in the situation of bone ingrowth ($\dot{\alpha} > 0$), $Y\dot{\alpha}$ is now positive and provides the rate of metabolic energy that the organism must supply to sustain the formation of new bone and the subsequent increase in the stiffness of the interface (see [Doblaré and García (2001, 2002)] for an equivalent interpretation in bone remodelling).

Damage/repair characterization

Now the evolution of the internal variable α must be established. In the models of previous sections, a single criterion in each direction β was sufficient to fully characterise the evolution of damage, since d could only increase or remain constant. Nevertheless, two appropriate criteria will be needed in this model, since we must now determine if α is increasing (bone ingrowth), decreasing (damage) or is not varying (dead or equilibrium zone). Moreover, we also consider that there exist two different mechanisms of evolution, each one acting in one direction, normal and shear, respectively.

Since the mechanical behaviour of bone-implant interface is usually similar in all the tangential directions, the formulation is established in terms of the normal and the total tangential components of the traction vector and the corresponding relative displacements, which are denoted by subscripts $(\cdot)_N$ and $(\cdot)_T$, respectively. Thus, two functions f_β^{dam} defining the damage criterion, two functions f_β^{ing} defining the bone ingrowth criterion and the law of the internal variable evolution $\dot{\alpha}$ has to be defined.

In the case of damage, the same yield functions and rate-independent damage evolution law proposed in Section 2.1.1. are used here, just replacing d by $1-\alpha$:

$$f_\beta^{dam}(Y_\beta,\alpha) = \alpha\sqrt{2K_{0\beta}Y_\beta} - t_\beta^u\left(\sqrt{\frac{2Y_\beta}{K_{0\beta}}}\right) \qquad \beta = N,T \tag{26}$$

where $K_{0N} = K_{01}$, $K_{0T} = K_{02} = K_{03}$ and t_β^u was defined in Eq.6.

In the case of bone ingrowth, instead of a rate-independent law of evolution, we propose the use of a viscous formulation, in the same way as in classical viscoplasticity [Simo and Hughes (1998); Simo (1998)] or viscodamage [Ju (1989)]. We recall that the main feature of this type of models is that, in sharp contrast with the situation found in rate-independent internal variable models, the stress state is no longer constrained to lie within the closure of the elastic range —what implies that the corresponding yield function can take positive values— and that the consistency parameter of the evolution law is no longer determined by the fulfillment of the consistency condition, like in the rate-independent case, but by means of a constitutive equation.

In our case, we use of the following functions f_β^{ing} to establish the bone ingrowth criterion:

$$f_\beta^{ing}(Y_\beta,\alpha) = t_\beta^{ing}(\alpha) - \alpha\sqrt{2K_{0\beta}Y_\beta} \qquad \beta = N,T \tag{27}$$

where $t_\beta^{ing} = \alpha K_{0\beta}\delta^{ing}$, being δ^{ing} a new parameter of the model with units of displacement.

Note that the bone ingrowth criterion presents a very clear physical interpretation: f_β^{ing} changes of sign when $\delta_\beta = \delta^{ing}$, being positive when $\delta_\beta < \delta^{ing}$ and negative when $\delta_\beta > \delta^{ing}$ (see Fig. 6). Therefore, δ^{ing} can be interpreted as the threshold in the jump of displacements across the interface, under which new bone can be deposited. This criterion is in complete agreement with numerous clinical experiments performed in humans and animals that confirm the well-established fact that bone ingrowth can only take place on the condition that the micromotion between implant and bone does not exceed a certain value (30 μm, for example) [Pilliar, Lee, and Maniatopoulos (1986); Sugiyama, Whiteside, and Kaiser (1989); Sϕballe, Brockstedt-Rasmussen, Hansen, and Bünger (1992); Sϕballe, Hansen, Brockstedt-Rasmussen, Jϕrgensen, and Bünger (1992); Sϕballe, Hansen, Brockstedt-Rasmussen, and Bünger (1993); Jasty, Bragdon, Zalenski, O'Connor, Page, and Harris (1997)].

Note also that under compression $f_N^{ing} > 0$ always holds, since Y_N is zero in this case and t_N^{ing} is positive.

Next, an evolutive law for the internal variable is suggested:

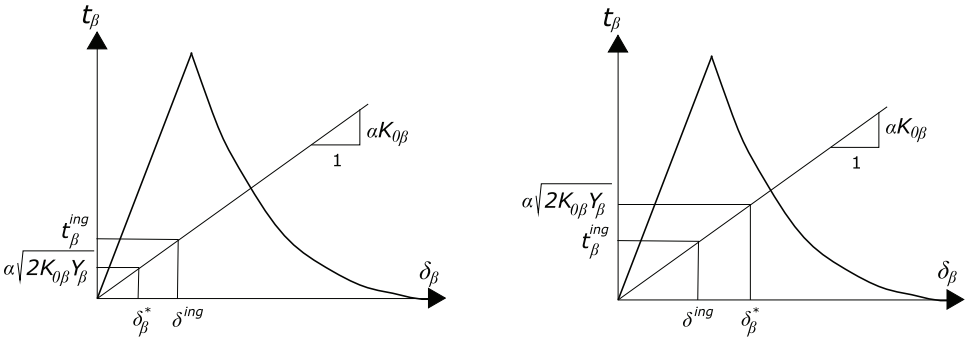

Figure 6: Bone ingrowth criterion: (a) bone ingrowth case, $f_\beta^{ing} > 0 \Rightarrow \dot{\alpha} > 0$; (b) Absence of bone ingrowth $f_\beta^{ing} < 0$.

$$\dot{\alpha} = \min_\beta \left\{ \mu_\beta^{dam} \frac{\partial f_\beta^{dam}}{\partial Y_\beta} + \mu_\beta^{ing} \frac{\partial f_\beta^{ing}}{\partial Y_\beta} \right\} \qquad \beta = N, T \tag{28}$$

μ_β and γ_β are consistency parameters in direction β in the case of damage and bone ingrowth, respectively.

Some remarks must be made regarding Eq.28. First, we must emphasise that the choice of criteria (26) and (27) prevents that bone ingrowth and damage can take place at the same time in a certain direction, what would not make sense from a mathematical standpoint. Hence, the consistency parameters μ_β^{dam} and μ_β^{ing} will never take values different than zero simultaneously for a certain β. The reason is that the experimentally obtained values of δ^{ing} [Sϕballe, Brockstedt-Rasmussen, Hansen, and Bünger (1992); Sϕballe, Hansen, Brockstedt-Rasmussen, Jϕrgensen, and Bünger (1992); Jasty, Bragdon, Zalenski, O'Connor, Page, and Harris (1997)] are always lower than the typical values of $\delta_{0\beta}$ (the relative displacement corresponding to the peak traction, as can be seen in Fig. 2 and criterion (26)) and thus it is clear that f_β^{dam} and f_β^{ing} cannot take positive values at the same time.

Secondly, it is possible, from a mathematical point of view, a condition in which the damage criterion is activated in one direction, whereas the bone ingrowth is in the other. In this case, the evolution law (28) simply drives to the lower value of $\dot{\alpha}$, that in this case is, the one corresponding to damage, since $\dot{\alpha} < 0$ in the case of damage.

Therefore, we have to keep in mind that it is not the aim of this phenomenological model to reproduce all the individual phenomena characteristic of the bone-implant interface at the local level, but to account for the macroscopic effect of the whole of them. Therefore, when damage (bone ingrowth) is taking place, it simply means that the net effect of the whole set of complex biological processes taking place at the interface is a decrease (increase) of the macroscopic mechanical properties.

After discussing some properties of the internal variable evolution law, we proceed with the determination of the consistency parameters. In the case of damage, the loading/unloading (Kuhn-Tucker) conditions that control the evolution of α read as follows

$$\mu_\beta^{dam} \geq 0; \quad f_\beta^{dam} \leq 0; \quad \mu_\beta^{dam} f_\beta^{dam} = 0 \qquad \beta = N, T \tag{29}$$

Observe the different sign of μ_β^{dam} with respect to (13), due to the change $\alpha = 1 - d$. As in Section 2.1.1, no damage can occur under compression since in this case $Y_N = 0$ and $f_\beta^{dam} < 0$.

By means of the use of the consistency conditions, we can obtain the counterpart expressions of (14a) and (14b) for the consistency parameters when a certain damage mechanism β is activated:

$$\mu_N^{dam} = -\dot{\delta}_1 \tag{30a}$$

$$\mu_T^{dam} = -\frac{\delta_2 \dot{\delta}_2 + \delta_3 \dot{\delta}_3}{\sqrt{\delta_2^2 + \delta_3^2}} = -\dot{\delta}_T \tag{30b}$$

As for bone ingrowth, if it were the case of a rate-independent model, we could straightforwardly determine the consistency parameters as

$$\mu_\beta^{ing} = \left(1 - \frac{\delta^{ing}}{\delta_\beta}\right)^{-1} \qquad \beta = N, T \tag{31}$$

However, as it is usual in rate-dependent models, the internal variable evolution law is directly postulated. In the present model, the following expression is proposed for the evolution of α in the case of bone ingrowth:

$$\mu_\beta^{ing} \frac{\partial f_\beta^{ing}}{\partial Y_\beta} = \begin{cases} \nu\alpha(\delta^{ing} - \delta_\beta) & \text{if } f_\beta^{ing} > 0 \text{ and } \alpha < 1 \\ 0 & \text{otherwise} \end{cases} \qquad \beta = N, T \tag{32}$$

which is equivalent to define the consistency parameter μ_β^{ing} as

$$\mu_\beta^{ing} = \begin{cases} \nu(\delta^{ing} - \delta_\beta)\sqrt{\frac{2Y_\beta}{K_{0\beta}}} & \text{if } f_\beta^{ing} > 0 \text{ and } \alpha < 1 \\ 0 & \text{otherwise} \end{cases} \qquad \beta = N, T \tag{33}$$

Fatigue damage

Cyclic loading can affect the process of damage, contributing to the growth of microcracks, but can also alter many features of cell behaviour, such as the rate of matrix secretion by osteoblasts, what definitely influences bone ingrowth. However, these two possible effects are still far from being quantitatively characterised through experiments, so its consideration in a mathematical model of this type is quite difficult. For this reason, we have decided to ignore the influence of cyclic loading on bone ingrowth, but to consider fatigue damage evolution in a simple manner by means of the previously used Miner's rule:

$$\dot{\alpha}^{cyc} = \frac{d}{dt}(\alpha) = \frac{d}{dn}(\alpha)\frac{d}{dt}(n) = -max\left\{\frac{1}{N_N^F}, \frac{1}{N_T^F}\right\} f \tag{34}$$

where we have assumed that N_N^F and N_T^F can be estimated in the same way as in (Moreo, Pérez, García-Aznar, and Doblaré (2006)) and t stands for time, n for cycles and f for the load frequency.

Contact

It is necessary to incorporate contact between the surfaces of bone and implant. The reasons that motivate the inclusion of this contact are two. The first one is related with the avoidance of penetration of adjacent points of bone and cement under high compressive loads. Secondly, contact is needed because when the interface still retains a significant part of its initial stiffness, tangential stresses are transmitted thanks to the mechanical cohesion of the interface itself. However, as the interface degrades and its stiffness approaches to zero, shear stresses cannot be longer supported and are now transferred by means of friction. In this case we use a Coulomb frictional model that only acts when the bonding degree α is lower than a threshold value $\alpha_0 = 0.4$, being the friction coefficient μ defined by the following expression:

$$\begin{cases} 0 \le \alpha \le \alpha_0 & \mu = \mu_0\left(1 - \frac{\alpha}{\alpha_0}\right) \\ \alpha_0 \le \alpha \le 1 & \mu = 0 \end{cases} \tag{35}$$

3.1.2 Example of application

The goal of this example is to reproduce by means of computational simulations the clinical experiments of ossoeintegration of dental implants in rabbit tibiae of Huang, Cheng, Chen, Lin, and Lee (2005) and verify if the model proposed in this section yields results in quantitative agreement with them [Pérez, Moreo, García-Aznar, and Doblaré (2008)].

The FE model of a rabbit tibia (see Fig. 7) was developed from a set of CT scans distinguishing between cortical and trabecular bone. The titanium dental implant used experimentally was 3.2 mm in diameter and 8 mm in length. Experimentally, a healing abutment was used to directly mount the device design to measure the resonance frequency. Therefore, in the FE model it has been included as a cylinder with the implant diameter and a length of 4.2 mm, and additional mass of 0.6g [Pérez, Moreo, García-Aznar, and Doblaré (2008)]. The implant was positioned in the tibia, following the experimental work of Huang, Cheng, Chen, Lin, and Lee (2005), in the proximal metaphysis, just in the mesiodistal direction (see Fig. 7). The values of the mechanical parameters of the interface model were obtained from different experimental results [Lin, Xu, Zhang, and de Groot (1998); Müller, Hennig, Hothorn, and Stangl (2006)].

Two types of analyses were performed. The healing activity during 1 week was simulated in order to compute the osseointegration evolution. During the healing, the rabbit activities per day were simulated (resting time, maintenance, investigate and abnormal behaviour, and locomotion). Then, the implant stability was evaluated through the determination of the resonance frequency. These two analyses were repeated 12 times, representing therefore a period of 12 weeks of healing. More details about the FE model and loading conditions can be found in Pérez, Moreo, García-Aznar, and Doblaré (2008).

The evolution of the resonance frequency associated to the first vibration mode during the simulation has been represented in Fig. 8. Within the first week after implantation, the slope of the curve is very low, but after that moment the resonance frequency increases steadily until around 7-8 weeks, when it reaches a maximum value of 4500 Hz, that remains constant till the end of the healing period. In the same figure it has been superimposed the evolution of resonance frequencies obtained experimentally [Huang, Cheng, Chen, Lin, and Lee (2005)]. Actually, a very nice quantitative agreement was found between the computational and the experimental curves.

The fact that the mathematical model is able to reproduce this slow initial bone ingrowth phase is simply due to the use of a law for $\dot{\alpha}$ that depends linearly on α (Eq.32). This provokes that in the early stages on healing, when α is small, the

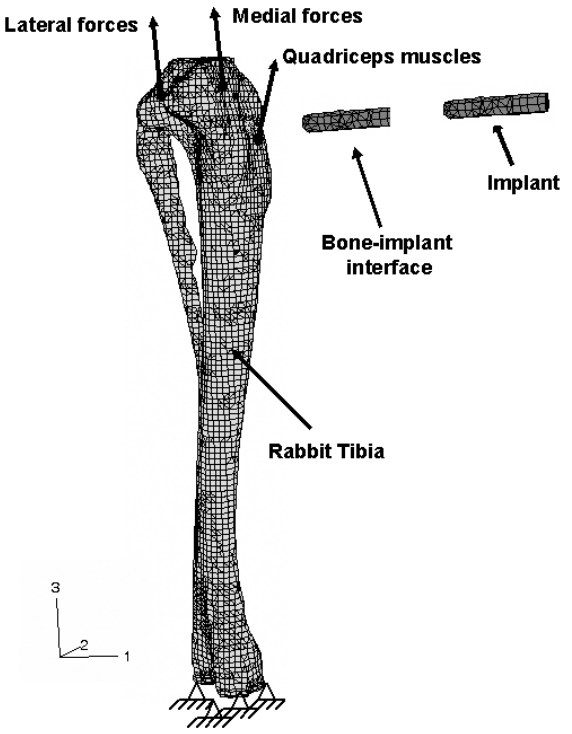

Figure 7: FE model of the tibia with the dental implant embedded proximally. The boundary and loading conditions are shown (with permission from Pérez, Moreo, García-Aznar, and Doblaré (2008)).

velocity of osseointegration is also small. Actually, it was first tried to reproduce these experiments using a law that did not depend on α achieving poor results, since the model predicted an excessive formation of bone in the first weeks. After this early phase, a second interval where the frequency increases abruptly follows. It is in this phase where new bone is formed. Note that from the whole period of 12 weeks, this phase only stretches from about the third week till the eighth week. Finally, when some regions of the interface begin to achieve a fully bonded situation, the resonance frequency of the interface starts to increase more slowly until reaching a plateau both in the experiment and the simulation.

Summarizing, the proposed approach is a phenomenological model able to study the influence of purely mechanical factors (i. e. geometry, stiffness) on the process of osseointegration.

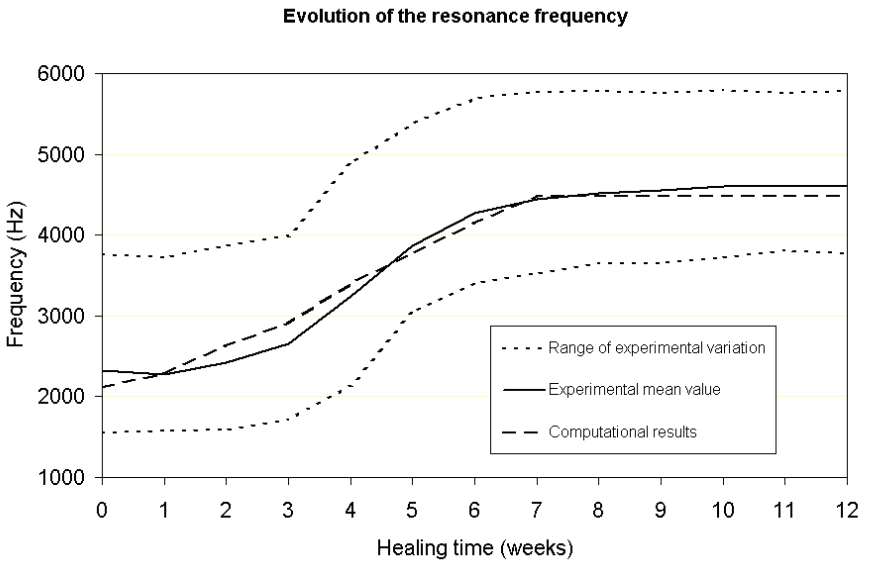

Figure 8: Healing curve plot of RF values predicted by the computational simulation (with permission from Pérez, Moreo, García-Aznar, and Doblaré (2008)).

3.2 Multiphysics and multiscale modelling of interfaces: a mechanistic approach

The phenomenological approach previously described allows obtaining results of high practical and clinical interest, but these models do not give information of how individual cells behave and how mechanical factors regulate the processes. However, mechanistic-based approaches allow incorporating the interaction among cells, tissue and biomaterial that regulate the biological events involved in the gap between bone and implant.

A brief summary of the main biological features that occurs after surgical implantation is now described (a detailed description can be found in Davies (2003); Puleo and Nanci (1999). Initially, just after surgical placement of the implant inside the host bone, a blood clot is formed around the implant through a coagulation process. Next, an inflammation phase is produced where necrotic bone tissue is eliminated by macrophages. Then, mesenchymal stem cells migrate from the surface of the old bone towards the implant. If the mechanical and biological conditions are adequate, they may differentiate into osteoblasts, which will start laying down bone matrix that will eventually remodel into mature lamellar bone. A less preferable situation corresponds to a differentiation of stem cells into fibroblasts since in this

case the implant will be encapsulated by a fibrous layer. This typically occurs in cases of excessive early relative motion.

The factors that regulate all these events are numerous and very complex, although they could be simplified in three:

1. Mechanical factors: the application of early loading in the implant may damage the granulation tissue, which limits the cell migration and differentiation and the corresponding extracellular matrix synthesis;

2. The properties of the implant or scaffold surface: the micro-topography and chemical properties of the implant are very important because can improve the protein adhesion and accelerate the implant integration;

3. Biochemical factors are also very important, because they can regulate signaling processes in cell processes.

Therefore, computational modelling of these processes requires the combination of multiple simultaneous biophysical phenomena, which is normally known as multiphysics analysis.

Moreover, all these factors interact at different temporal and spatial scales. In fact, when a load is applied in the implant, this load is transferred to the living tissue that surrounds the implant. Then, this load-bearing tissue is synthesized, regenerated, and adapted by cells as response to this mechanical stimulus. Therefore, the load that supports the implant is acting at the organ level and its rate of application is in the order of seconds, whereas the cell response occurs at cellular level depending on the mechanical stimulus that the cell sense at this level and the response rate of the cell is clearly slower (the order of days). Therefore, the complete modelling of these processes requires the use of different scales (at least two: organ and cellular level), that allows exploring mechanotransduction at the cellular level and carry the information all the way up to the organ scale.

4 Discussion and conclusions

In this work, we have shown the potential of interface modelling in biomechanics with a simple interface model. In spite of the lack of experimental data characteristics in biological systems biomechanical models allow to perform qualitative analysis with significant conclusions.

In fact, the model here presented is very simple and, however results are significant. In any case, this simple model can be easily improved and extended, incorporating additional effects: using more state variables, such as for example the per-

manent slide experimentally observed on cement-bone interface [Moreo, García-Aznar, and Doblaré (2007)]; using more complex and realistic models like the poroelastic behaviour characteristic of bone tissue [Cowin (1999)] or its adaptative properties [Huiskes, Weinans, Grootenboer, Dalstra, Fudala, and Slooff (1987)]; modelling contact mechanics with an approach more precise [Jackson and Kogut (2006); Pugliese, Tavares, Ciulli, and Ferreira (2008)].

As we have shown in this work, these biomechanical models are valid when we are only interested on the passive mechanical behaviour of the interface. However, in biological systems, interfaces are living and present an active characteristic that imply an evolutive behaviour of the interface mechanical properties. Therefore, its modelling requires to incorporate additional effects as, for example, to describe how the mechanical factors interact with biological processes, what is normally known as *mechanobiology* [van der Meulen and Huiskes (2002)]. From a computational point of view, two different approaches are normally used in computational mechanobiology: phenomenological or mechanistic. In the first one, the aim is to predict the macroscopic properties of the interface independently of the biological processes here involved. In this work we have presented a simple model with this idea to simulate osseointegration around a prosthesis. This model is based on the extension of a classical cohesive interface model that incorporate both effects damage and repair. Whereas, in the case of a mechanistic approach a more profound analysis is required, with the purpose of studying and understanding how the mechanical factors influence and regulate the evolution of the biological processes and therefore how these control the mechanical properties evolution. A detailed description of the main aspects that are necessary to develop interface models based on a mechanistic approach is performed in this work, concluding that these kind of models require the development of more complex and sophisticated computational models that include multi-scale and multi-physics approaches.

Acknowledgement: The authors would like to thank to the CIBER-BBN Centro de Investigación en Red en Bioingeniería, Biomateriales y Nanomedicina - IACS - Aragón Institute of Health Sciences and to the research support of the Aragón Goverment through the Research Project DGA PI031/08.

References

Ambard, D.; Swider, P. (2006): A predictive mechano-biological model of the bone-implant healing. *Eur. J. Mech. A-Solids*, vol. 25, pp. 927–937.

Andreykiv, A.; Prendergast, P. J.; van Keulen, F.; Swieszkowski, W.; Rozing, P. M. (2005): Bone ingrowth simulation for a concept glenoid component design.

J Biomech, vol. 38, pp. 1023–1033.

Büchler, P.; Pioletti, D. P.; Rakotomanana, L. R. (2003): Biphasic constitutive laws for biological interface evolution. *Biomechan Model Mechanobiol*, vol. 1, pp. 239–249.

Camacho, G. T.; Ortiz, M. (1996): Computational modelling of impact damage in brittle materials. *Int. J. Solid. Struct.*, vol. 33 (20-22), pp. 2899–2938.

Canale, S. T. (2003): *Campbell's Operative Orthopaedics,*, pp. 1481–1503. 2003.

Chandra, N.; Shet, C. (2004): A micromechanistic perspective of cohesive zone approach in modeling fracture. *CMES: Computer Modeling in Engineering & Sciences*, vol. 5(1), pp. 21–34.

Cocchetti, G.; Maier, G.; Shen, X. P. (2002): Piecewise linear models for interfaces and mixed mode cohesive cracks. *CMES: Computer Modeling in Engineering & Sciences*, vol. 3(3), pp. 279–298.

Cohen, B.; Chorney, G. S.; Phillips, D. P.; Dick, H. M.; Buckwalter, J. A.; Ratcliffe, A.; Mow, V. C. (1992): The microstructural tensile properties and biochemical composition of the bovine distal femoral growth plate. *J. Orthop. Res.*, vol. 10(2), pp. 263–275.

Coleman, B. D.; Gurtin, M. E. (1967): Thermodynamics with internal state variables. *J Chem Phys*, vol. 47, pp. 597–613.

Coleman, B. D.; Noll, W. (1963): The thermodynamics of elastic materials with heat conduction and viscosity. *Arch Rational Mech Anal*, vol. 13, pp. 167–178.

Collis, D. K.; Mohler, C. G. (2002): Comparison of clinical outcomes in total hip arthroplasty using rough and polished cemented stems with essentially the same geometry. *J Bone Joint Surg*, vol. 84, pp. 586–592.

Cowin, S. (1999): Bone poroelasticity. *J Biomech*, vol. 32, pp. 217–238.

Davies, J. E. (2003): Understanding peri-implant endosseous healing. *J. Dental Educ.*, vol. 67, pp. 932–949.

Doblaré, M.; García, J. (2001): Bone remodelling analysis of the proximal femur after total hip replacement and implantation of an exeter prosthesis. *J. Biomech.*, vol. 34(9), pp. 1157–1170.

Doblaré, M.; García, J. M. (2002): Anisotropic bone remodelling model based on a continuum damage-repair theory. *J. Biomech.*, vol. 35(1), pp. 1–17.

Fernandes, P. R.; Folgado, J.; Jacobs, C.; Pellegrini, V. (2002): A contact model with ingrowth control for bone remodelling around cementless stems. *J Biomech*, vol. 35, pp. 167–176.

Fishkin, Z.; Armstrong, D. G.; Shah, H.; Patra, A.; Mihalko, W. M. (2006): Proximal femoral physis shear in slipped capital femoral epiphysis - a finite element study. *J. Pediatr. Orthop.*, vol. 26(3), pp. 291–294.

Fornasier, V. L.; Cameron, H. U. (1976): The femoral stem/cement interface in total hip replacement. *Clin Orthop Rel Res*, vol. 116, pp. 248–252.

Geris, L.; Andreykiv, A.; Oosterwyck, H. V.; Sloten, J. V.; van Keulen, F.; Duyck, J.; Naert, I. (2004): Numerical simulation of tissue differentiation around loaded titanium implants in a bone chamber. *J. Biomech.*, vol. 37, pp. 763–769.

Gómez-Benito, M. J.; Moreo, P.; Pérez, M. A.; Paseta, O.; García-Aznar, J. M.; Barrios, C.; Doblaré, M. (2007): A damage model for the growth plate: Application to the prediction of slipped capital epiphysis. *J Biomech*, vol. 40, pp. 3305–3313.

Gómez-Benito, M. J.; Paseta, O.; García-Aznar, J. M.; Barrios, C.; Gascó, J.; Doblaré, M. (2006): Biomechanical Analysis of a Slipped Capital Femoral Epiphysis. In Baldini, N.; Savarino, L.(Eds): *EORS 2006 Bologna 16th Annual Meeting Transactions Vol. 16*, pg. 98. Italian Orthopaedic Research Society.

Harris, W. H. (1992): Is it advantageous to strengthen the cement-metal interface and use a collar for cemented femoral components of total hip replacement? *Clin Orthop*, vol. 285, pp. 67–72.

Huang, H. M.; Cheng, K. Y.; Chen, C. H.; Lin, C. T.; Lee, S. Y. (2005): Design of a stability-detecting device for dental implants. *Proceedings of the Institution of Mechanical Engineering - Part H - Journal of Engineering in Medicine*, vol. 219, pp. 203–211.

Huiskes, R.; Verdonschot, N.; Nivbrant, B. (1998): Migration, stem shape and surface finish in cemented total hip arthroplasty. *Clin Orthop Rel Res*, vol. 355, pp. 103–112.

Huiskes, R.; Weinans, H.; Grootenboer, H. J.; Dalstra, M.; Fudala, B.; Slooff, T. J. (1987): Adaptive bone-remodeling theory applied to prosthetic-design analysis. *J Biomech*, vol. 20(11-12), pp. 1135–1150.

Irwin, G.; Kies, J.; Smith, H. (1958): Fracture strengths relative to onset crack propagation. In *Proceedings of the American Society for Testing Materials*, pp. 640–657.

Jackson, R. L.; Kogut, L. (2006): A comparison of flattening and indentation approaches for contact mechanics modeling of single asperity contacts. *J. Tribol.*, vol. 128, pp. 209.

Jasty, M.; Bragdon, C. R.; Zalenski, E.; O'Connor, D.; Page, A.; Harris, W. H. (1997): Enhanced Stability of Uncemented Canine Femoral Components by Bone Ingrowth Into the Porous Coatings. *J Arthroplasty*, vol. 12(1), pp. 106–113.

Jasty, M.; Maloney, W. J.; Bragdon, C. R.; O'Connor, D. O.; Haire, T.; Harris, W. H. (1991): The initiation of failure in cemented femoral components of hip arthroplasties. *J Bone Joint Surg*, vol. 73-B, pp. 551–558.

Ju, J. W. (1989): On energy-based coupled elastoplastic damage theories: constitutive modeling and computational aspects. *Int. J. Solids Struct.*, vol. 25, no. 7, pp. 803–833.

Kasemo, B. (1998): Biological surface science. *Curr Opin Solid State Mat Sci*, vol. 3, pp. 451–459.

Kim, D. G.; Miller, M. A.; Mann, K. A. (2004): A fatigue damage model for the cement-bone interface. *J Biomech*, vol. 37, pp. 1505–1512.

Kim, D. G.; Miller, M. A.; Mann, K. A. (2004): Creep dominates tensile fatigue damage of the cement-bone interface. *J Orthop Res*, vol. 22, pp. 633–640.

Lee, K. E.; Pelker, R. R.; Rudicel, S. A.; Ogden, J. A.; Panjabi, M. M. (1985): Histologic patterns of capital femoral growth plate fracture in rabbit: the effect of shear direction. *J Pediatr Orthop*, vol. 5, pp. 32–39.

Lennon, A. B.; Prendergast, P. J. (2001): Evaluation of cement stresses in finite element analyses of cemented orthopaedic implants. *J Biomech Eng*, vol. 123, no. 6, pp. 623–628.

Li, W.; Siegmund, T. (2004): Numerical study of indentation delamination of strongly bonded films by use of a cohesive zone model. *CMES: Computer Modeling in Engineering & Sciences*, vol. 5(1), pp. 81–90.

Lin, H.; Xu, H.; Zhang, X.; de Groot, K. (1998): Tensile tests of interface between bone and plasma-sprayed HA coating-titanium implant. *J. Biomed. Mater. Res. (Appl. Biomater.)*, vol. 43, pp. 113–122.

Liu, X.; Niebur, G. L. (2008): Bone ingrowth into a porous coated implant predicted by a mechano-regulatory tissue differentiation algorithm. *Biomechan. Model. Mechanobiol.*, vol. 7, pp. 335–344.

Loder, R. T. (1996): The demographics of slipped capital femoral epiphysis. an international multicenter study. *Clin Orthop Relat Res*, vol. 322, pp. 8–27.

Loder, R. T. (1998): Slipped capital femoral epiphysis. *Am Fam Physician*, vol. 57(9), pp. 2135–42.

Luenberger, D. G. (1984): *Linear and Nonlinear Programming*. Addison-Wesley Publishing Company, Reading, Mass.

Mann, K. A.; Bartel, D. L.; Wright, T. M.; Burstein, A. H. (1995): Coulomb frictional interfaces in modeling cemented total hip replacements: A more realistic model. *J Biomech*, vol. 28(9), pp. 1067–1078.

Müller, M.; Hennig, F. F.; Hothorn, T.; Stangl, R. (2006): Bone-implant interface shear modulus and ultimate stress in a transcortical rabbit model of open-pore Ti6Al4V implants. *J. Biomech.*, vol. 39, pp. 2123–2132.

Mohler, C. G.; Callaghan, J. J.; Collis, D. K.; Johnston, R. C. (1995): Early loosening of the femoral component at the cement-prosthesis interface after total hip replacement. *J Bone Joint Surg*, vol. 77A, pp. 1315–1322.

Moreo, P.; García-Aznar, J. M.; Doblaré, M. (2007): A coupled viscoplastic rate-dependent damage model for the simulation of fatigue failure of cement-bone interfaces. *Int J Plast*, vol. 23(12), pp. 2058–2084.

Moreo, P.; García-Aznar, J. M.; Doblaré, M. (2009): Bone ingrowth on the surface of endosseous implants. part 1: Mathematical model. *J. Theor. Biol.*, pg. in press.

Moreo, P.; García-Aznar, J. M.; Doblaré, M. (2009): Bone ingrowth on the surface of endosseous implants. part 2: Theoretical and numerical analysis. *J. Theor. Biol.*, pg. in press.

Moreo, P.; Pérez, M. A.; García-Aznar, J. M.; Doblaré, M. (2006): Modelling the mixed-mode failure of cement-bone interfaces. *Eng Frac Mech*, vol. 73, no. 10, pp. 1379–1395.

Needleman, A. (1987): A continuum model for void nucleation by inclusion debonding. *J. Appl. Mech.*, vol. 54, pp. 525–531.

Needleman, A. (1990): An analysis of tensile decohesion along an interface. *J. Mech. Phys. Solids*, vol. 8, pp. 100–104.

Paseta, O.; Gómez-Benito, M. J.; García-Aznar, J. M.; Barrios, C.; Doblaré, M. (2007): Parametric geometrical finite element models of proximal femur: a tool to predict slipped capital femoral epiphysis. *International Journal for Computational Vision and Biomechanics*, vol. 1, pp. 1–9.

Pilliar, R. M.; Lee, J. M.; Maniatopoulos, C. (1986): Observations on the effect of movement on bone ingrowth into porous surfaced implants. *Clin. Orthop.*, vol. 208, pp. 108–113.

Pérez, M. A.; García-Aznar, J. M.; Doblaré, M.; Seral, B.; Seral, F. (2006): A comparative FEA of the debonding process in different concepts of cemented hip implants. *Med Eng Phys*, vol. 28, pp. 525–533.

Pérez, M. A.; Moreo, P.; García-Aznar, J. M.; Doblaré, M. (2008): Computational simulation of dental implant osseointegration through resonance frequency analysis. *J. Biomech.*, vol. 41(2), pp. 316–325.

Pugliese, G.; Tavares, S.; Ciulli, E.; Ferreira, L. (2008): Rough contacts between actual engineering surfaces: Part ii. contact mechanics. *Wear*, vol. 264(11-12), pp. 1116–1128.

Puleo, D. A.; Nanci, A. (1999): Understanding and controlling the bone-implant interface. *Biomater.*, vol. 20, pp. 2311–2321.

Race, A.; Miller, M. A.; Ayers, D. C.; Mann, K. A. (2003): Early cement damage around a femoral stem is concentrated at the cement/bone interface. *J Biomech*, vol. 36, pp. 489–496.

Simo, J. C. (1998): Topics on the numerical analysis and simulation of plasticity. In Ciarlet, P. G.; Lions, J. L.(Eds): *Handbook of Numerical Analysis*, volume III. Elsevier Science Publishers, Amsterdam North Holland.

Simo, J. C.; Hughes, T. J. R. (1998): *Computational Inelasticity*. Springer-Verlag, New York.

Sϕballe, K.; Brockstedt-Rasmussen, H.; Hansen, E. S.; Bünger, C. (1992): Hydroxiapatite coating modifies implant membrane formation. *Acta Orthop. Scand.*, vol. 63(2), pp. 128–140.

Sϕballe, K.; Hansen, E. S.; Brockstedt-Rasmussen, H.; Bünger, C. (1993): Hydroxyapatite coating converts fibrous tissue to bone around loaded implants. *J. Bone Joint Surg.*, vol. 75-B, pp. 270–278.

Sϕballe, K.; Hansen, E. S.; Brockstedt-Rasmussen, H.; Jϕrgensen, P. H.; Bünger, C. (1992): Tissue ingrowth into titanium and hydroxyapatite-coated implants during stable and unstable mechanical conditions. *J. Orthop. Res.*, vol. 10, pp. 285–299.

Stolk, J.; Verdonschot, N.; Huiskes, R. (2001): Hip-joint and abductor-muscle forces adequately represent in vivo loading of a cemented total hip reconstruction. *J Biomech*, vol. 34, pp. 917–926.

Stone, M. H.; Wilkinson, R.; Stother, I. G. (1989): Some factors affecting the strength of the cement-metal interface. *J Bone Joint Surg (Br)*, vol. 71, pp. 217–221.

Sugiyama, H.; Whiteside, L. A.; Kaiser, A. D. (1989): Examination of rotational fixation of the femoral component in total hip arthoplasty. A mechanical study of micromovement and acoustic emission. *Clin. Orthop.*, vol. 249, pp. 122–128.

van der Meulen, M.; Huiskes, R. (2002): Why mechanobiology? *J Biomech*, vol. 35(4), pp. 401–414.

Van Oosterwyck, H.; Duyck, J.; Vander Sloten, J.; Van der Perre, G.; Cooman, M. D.; Lievens, S.; Puers, R.; Naert, I. (1998): The influence of bone mechanical properties and implant fixation upon bone loading around oral implants. *Clin Oral Impl Res*, vol. 9, pp. 407–418.

Williams, J. L.; Do, P. D.; Eick, J. D.; Schmidt, T. L. (2001): Tensile properties of the physis vary with anatomic location, thickness, strain rate and age. *J. Orthop. Res.*, vol. 19, pp. 1043–1048.

Williams, J. L.; Vani, J. N.; Eick, J. D.; Petersen, E. C.; Schmidt, T. L. (1999): Shear strength of th physis varies with anatomic location and is a function of modulus, inclination and thickness. *J. Orthop. Res.*, vol. 17, pp. 214–222.

Zhong, Z.-H.; Mackerle, J. (1992): Contact-impact problems: a review with bibliography. *Eng. Comput.*, vol. 9, pp. 3–37.

Zhong, Z.-H.; Mackerle, J. (1994): Static contact problems-a review. *ASME Trans. Appl. Mech. Rev*, vol. 47 (2), pp. 55–76.